Quench dynamics across topological quantum phase transitions

Shiuan-Fan Liou and Kun Yang

Quench Dynamics Across Topological Quantum Phase Transitions

Shiuan-Fan Liou[1] and Kun Yang[1]

[1]*National High Magnetic Field Laboratory and Physics Department,*
Florida State University, Tallahassee, FL 32306, USA
(Dated: June 14, 2018)

We study the dynamics of systems quenched through topological quantum phase transitions and investigate the behavior of the bulk and edge excitation with various quench rates. Specifically, we consider Haldane model and checkerboard model in slow quench processes with distinct band touching structures leading to topology changes. The generation of bulk excitations is found to obey the power-law relation Kibblle-Zurek and Landau-Zener theories predict. However, an anti-Kibble-Zurek behavior is observed in the edge excitations. The mechanism of excitation generation on edge states is revealed, which explains the anti-Kibble-Zurek behavior.

I. INTRODUCTION

The non-equilibrium dynamics of systems undergoing phase transitions is an important subject in statistical physics. In particular, quench dynamics through both classical and quantum second-order phase transitions involving symmetry breaking has been of great interest. Kibble-Zurek (KZ) mechanism, a theory originally developed in the study of formation of the topological defects in the early universe[1,2], was applied to quench dynamics near symmetry breaking second-order phase transitions[3–5], and provided a fairly accurate prediction of a power-law relation between the topological defect density and the quench rate[6]. In the meanwhile, Landau-Zener (LZ) theory[7] describing a two-level transition was also applied to the study of dynamics of quantum phase transitions where applicable, yielding results[8,9] consistent with KZ theory. Some systems under inhomogeneous quench[10] and non-linear quench[11,12] out of the scope of KZ mechanism have been investigated as well.

In the contrary, non-equilibrium dynamics across topological phase transitions that do not involve symmetry breaking has been studied much less. Topological phases of matter are of tremendous importance and current interest[13]. Some fundamental questions about the dynamics of topological phase transitions naturally arise. First, since there is no symmetry breaking in such phase transitions, can KZ theory effectively describe their dynamics? Second, what is the mechanism of topological defect generation, and how is it related to the symmetry breaking case? Among many unique properties of topological states, of particular importance is the presence of robust edge states that often give rise to dissipationless and quantized transport; they have been proposed to be the building blocks of electronic devices with low or even zero dissipation[14,15]. Operating such devices often involves switching between topologically trivial (the insulating or off) state and non-trivial (conducting or on) states. Thus understanding quench dynamics across topological phase transitions, especially its impact on edge states, is of both fundamental and practical importance. While there exist some reports on such studies[16–28], a comprehensive understanding has yet to emerge, especially when edge states are involved.

In this work, we study quench dynamics across topological quantum phase transitions (TQPTs) in the simplest setting of free fermion systems. Since in ultra-cold atom field Haldane model can be realized through optical traps[29], which enables people to explore and access the phase diagram of Haldane model, some study about the sudden quench dynamics through various topological phase transitions on Haldane model has been demonstrated in ultra-cold atom experiments.[23] We believe the slow quench process on Haldane model is feasible because sudden quench is just a limit of a general quench process. Thus, here we specifically consider two models: Haldane model[30] and checkerboard model[31,32] with linear and quadratic band dispersions at the gap closing points (where the TQPTs occur) respectively. The TQPTs result in changes of band Chern numbers by one and two respectively, and appearance of edges states in the former, and reverse of edge state chirality in the latter. We numerically follow the time evolutions of the systems (initially in the ground states) under quenches that move the systems across the phase boundaries, and monitor the generation of excitations both in bulk and at the edge. We argue the bulk excitations are analogous to the topological defects in the case of symmetry-breaking phase transitions, and obtain results consistent with the prediction of KZ and LZ theories. Appearance of edge excitations, on the other hand, is unique to TQPTs and has no analogue in symmetry-breaking phase transitions. A particularly interesting finding that we report here is an anti-KZ behavior, namely the number of edge excitations depends on quench rate non-monotonically. We will provide an explanation of this counter-intuitive result.

The rest of this paper is organized as follows: in Sec. II, we introduce the two models, Haldane model and checkerboard model, studied in this work. In Sec. III, we briefly describe the concepts of Kibble-Zurek theory and Landau-Zener theory, derive the power-law relation between the (bulk) excitation density and the quench rate based on each theory, and use the results for our models. Before showing the results, in Sec. IV we describe the numerical methods of studying slow quench problems with edges and calculating bulk and edge excitations. We show our

results and have some discussions in Sec. V, in which the discussion and comparison with theoretical predictions of the bulk excitations are made in Sec. V A and the discussion of edge excitation and the mechanism of the excitation generation are included in Sec. V B. In Sec. VI we end the paper by offering some concluding remarks.

II. MODELS

In this section we introduce the models we study and their phase diagrams.

A. Haldane Model

Haldane model describes spinless fermions hopping on a honeycomb lattice with a real nearest neighbor (NN) hopping, a complex next nearest neighbor (NNN) hopping and an energy offset with a sign difference on the two sublattices. The Hamiltonian can be written as

$$
\begin{aligned}
H = &-\sum_{\langle i,j \rangle} \left(C^{\dagger}_{A,i} C_{B,j} + h.c. \right) \\
&+ \eta \sum_{\langle\langle i,j \rangle\rangle} \left[e^{iv_{ij}\phi} \left(C^{\dagger}_{A,i} C_{A,j} - C^{\dagger}_{B,i} C_{B,j} \right) + h.c. \right] \\
&+ m \sum_{i} \left(C^{\dagger}_{A,i} C_{A,i} - C^{\dagger}_{B,i} C_{B,i} \right),
\end{aligned}
\tag{1}
$$

where $C^{\dagger}_{\sigma,i}$ ($C_{\sigma,i}$) is the fermion creation (annihilation) operator, $\langle i,j \rangle$ and $\langle\langle i,j \rangle\rangle$ represent summing over the NNs and the NNNs, respectively, and A and B label the two sublattices. $v_{ij} \equiv \hat{z} \cdot \left(\hat{d}_j \times \hat{d}_i \right)$ with $\hat{z}$ the unit vector perpendicular to the two dimensional (2D) plane and $\{\hat{d}_i\}$ the unit vector along the bond connecting two nearest sites as shown in Fig. 1(a). The complex hopping with a phase $e^{iv_{ij}\phi}$ in the second term due to the staggered magnetic field breaks time reversal symmetry and the last term breaks spatial inversion symmetry.

As shown in the phase diagram[30] Fig. 1(c), we can access different topological phases by tuning parameters m, η and ϕ. In this study, we quench the system from the topologically trivial phase with Chern number $C = 0$ to the topologically non-trivial phase with $C = -1$ along the path (vertical dashed arrow) in Fig. 1(c), setting $\eta = \frac{1}{3}$ and $\phi = \frac{\pi}{2}$ ($|\eta| \leq \frac{1}{3}$ prevents band overlap)[30], by varying m from 3 to 0 linearly with time, namely, $m = 3 - \frac{t}{\tau}$ with $\frac{1}{\tau}$ the quench rate. When $m = \sqrt{3}$, the system reaches the phase boundary, and the energy gap in the bulk closes at the highly symmetric point (K or K') resulting in linear dispersion. Figs. 2(a) to (c) show the dispersions of $H(t)$ of Haldane model with zigzag edges in the x direction at the initial time, critical time and final time corresponding to no edge states, band touching and edge states popping up, respectively.

B. Checkerboard Model

Motivated by the Refs.[31,32], we consider a simplified checkerboard model with two sublattices (A and B) having a real and isotropic NN hopping, two kinds of non-trivial NNN hoppings and a complex NN hopping which leads to a quantum anomalous Hall (QAH) phase. The Hamiltonian is given by

$$
\begin{aligned}
H = &-\sum_{\vec{r},\vec{\delta}} C^{\dagger}_{A,\vec{r}} C_{B,\vec{r}+\vec{\delta}} + iV \sum_{\vec{\delta}} D_{\delta}\, C^{\dagger}_{A,\vec{r}} C_{B,\vec{r}+\vec{\delta}} \\
&- \xi' \sum_{\vec{r}} \left(C^{\dagger}_{A,\vec{r}} C_{A,\vec{r}\pm\vec{a}_1} + C^{\dagger}_{B,\vec{r}} C_{B,\vec{r}\pm\vec{a}_2} \right) \\
&- \xi'' \sum_{\vec{r}} \left(C^{\dagger}_{A,\vec{r}} C_{A,\vec{r}\pm\vec{a}_2} + C^{\dagger}_{B,\vec{r}} C_{B,\vec{r}\pm\vec{a}_1} \right) + H.c.,
\end{aligned}
\tag{2}
$$

where $\vec{a}_1 = \pm(0,a)$, $\vec{a}_2 = \pm(a,0)$, $D_{\vec{\delta}} = +1$ if $\vec{\delta} = \pm(a/2,a/2)$ and $D_{\vec{\delta}} = -1$ if $\vec{\delta} = \pm(a/2,-a/2)$ with $a/\sqrt{2}$ the lattice spacing. The first term represents the isotropic NN hopping. The second term is a purely imaginary NN hopping which is positive if hopping along arrows in Fig. 1(b) and picks up a minus sign otherwise, inducing QAH phase with non-trivial topology $C = \pm 1$. The last two terms correspond to the NNN hoppings along the red and the black cross lines [in Fig. 1(b)] with strengths ξ' and ξ'' respectively, which break C_4 symmetry if $\xi' \neq \xi''$.

A phase diagram of checkerboard model with only one relevant parameter V is provided in Fig. 1(d). In this model, we change the complex hopping strength V from 1 to -1 linearly, $V = 1 - \frac{t}{\tau}$, so that the Chern number C changes sign (from -1 to 1) indicated by the dashed arrow in Fig. 1(d) with $\xi' = -\xi'' = 0.5$. At $V = 0$, the gap in the bulk closes at $(k_x, k_y) = (\pi, \pi)$ with a quadratic dispersion as shown in Fig. 2(e). During the quench process, the dispersions of $H(t)$ with edges in the x direction at the initial, critical and final times are shown in Figs. 2(d) to (f). Since the system is quenched from one topologically non-trivial phase to another, edge states always exist during the whole process but their chirality is reversed. Note that one can also change the Chern number by two in Haldane model following the horizontal dotted path in Fig. 1(c). However, the gap closing will occur at two Dirac points K and K' instead of one, resulting in critical behavior distinct from the case in checkerboard model but similar to what happens when the gap closes at a single Dirac point discussed earlier.

III. THEORIES

In preparation for later comparisons, in this section we review the basics of Kibble-Zurek (KZ) and Landau-Zener (LZ) theories, and in particular discuss the relevance of the KZ theory to the topological phase transitions we study.
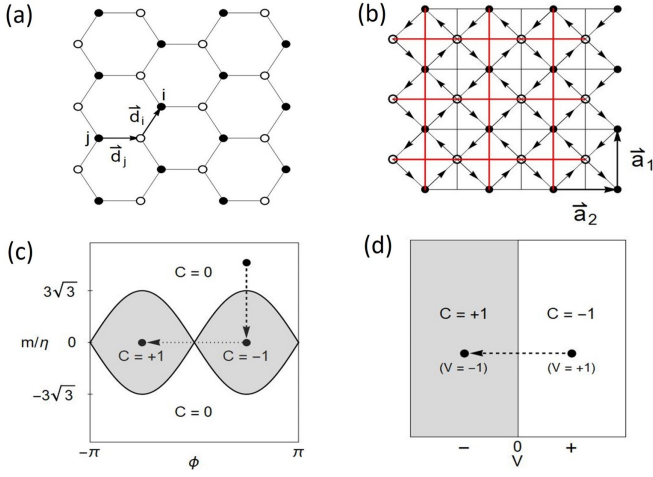
FIG. 1. (Color online) (a) Haldane model on honeycomb lattice. (b) Checkerboard model. The NNN hoppings along the red and the black cross lines have the hopping strength ξ' and ξ''; the imaginary strength of the NN hoppings following the directions of the arrows is positive and is negative otherwise. (c) Phase diagram of Haldane model. (d) Phase diagram of checkerboard model with only one relevant parameter V.
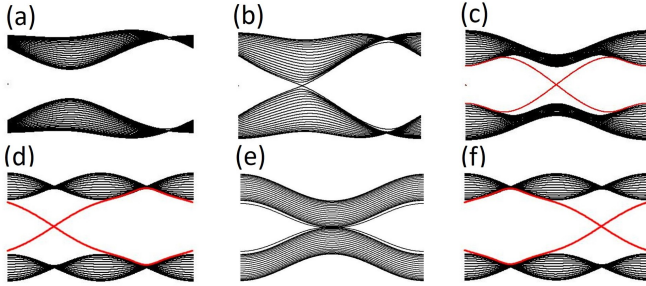

FIG. 2. (Color online) (a)-(c) Dispersions of Haldane model with zigzag edge at the initial time ($C = 0$), at the critical time when $m = \sqrt{3}$ with gap closing (linear dispersion) and at the final time ($C = 1$) having edge states (red curves). (d)-(e) Dispersions of Checkerboard model at the initial time ($C = -1$) having edge states on the left, at the critical time when $V = 0$ with gap closing (quadratic dispersion) and at the final time ($C = +1$) having edge states on the right. Edge states are the red curves.

A. Kibble-Zurek (KZ) theory

For a quench process which involves a second order phase transition from a high symmetry phase to a broken symmetry phase with gap closing at the critical point, the system can no longer evolve adiabatically due to the un-reachable relaxation time which is inversely proportional to the energy gap. KZ theory separates such a quench process into two regimes: adiabatic regime and impulsive regime as shown in Fig. 3. When the system enters the impulsive (diabatic) regime, the information of the system will be frozen because the relaxation time and the time scale of the quench are comparable. In such a quench process, (bulk) excitations (defects) are inevitable.

In the following, we derive the relation between the (bulk) defect density and the quench rate based on a linear quench assumption. For a second order phase transition, the energy gap Δ has a power-law relation with the quench parameter $\mu(t)$ with the critical point μ_c where the gap closes.

$$\Delta \sim |\frac{\mu(t)}{\mu_c} - 1|^{z\nu} \tag{3}$$

where z is the dynamic critical exponent and ν is the correlation length critical exponent. Moreover, the correlation length ξ has a power-law relation with the quench parameter as well and will blow up for infinite systems or be comparable to the system size for finite systems at the critical point.

$$\xi \sim |\frac{\mu(t)}{\mu_c} - 1|^{-\nu} \tag{4}$$

Assume that the quench process starts at $t = -\infty$, terminates at $t = \infty$, and the gap closes at $t = 0$. According to the linear quench assumption, we can define $\epsilon(t) \equiv \frac{\mu(t)}{\mu_c} - 1 \sim \frac{|t|}{\tau}$ with $\frac{1}{\tau}$ the quench rate. While the system enters the impulsive regime at the time $-\hat{t}$ as shown in Fig. 3, the relaxation time $\eta(-\hat{t})$ and the quench time scale $|\hat{t}|$ are comparable, namely,

$$\eta(-\hat{t}) = \frac{\hbar}{\Delta} \sim \hat{t}. \tag{5}$$

From Eq.(5) we can express $\hat{t}$ in terms of the quench rate $\frac{1}{\tau}$. From a high symmetry phase to a broken symmetry phase, the excitation size could be estimated through the correlation length as ξ^d in d-dimension space. Combining Eq.(3)-(5), therefore, we get the power-law relation of the excitation density n_{topo}, which is inversely proportional to the size of an excitation, and the quench rate

$$n_{topo} \sim \tau^{\frac{-d\nu}{1+z\nu}}. \tag{6}$$

The power-law relation in Eq.(6) has been shown with very good agreement with the numerical result studying the phase transitions associated with symmetry breaking.[6]

The topological phase transitions we are interested in in this work are second order phase transitions. Since there is no symmetry breaking in such transitions, it may not be obvious that the KZ theory is relevant here at the first glance. Those topological phases here are characterized by Chern numbers, and have one-to-one correspondences to (integer) quantum Hall states. As reviewed in Ref.[33], quantum Hall states can be mapped onto super-fluid states, in which composite bosons made of electrons and appropriate amount of flux condense and develop (quasi) long-range order. They are thus analogous to broken symmetry states. In particular, excitations (particles
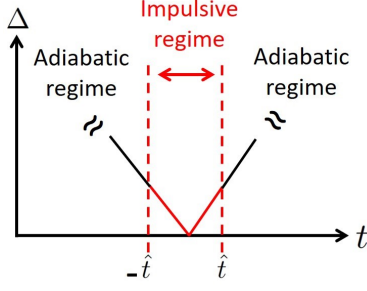
FIG. 3. (Color online) Schematic diagram for illustration of Kibble-Zurek theory. The energy gap of two states Δ is a function of time t. Within $t = -\hat{t}$ to $\hat{t}$, the system are in the impulsive regime in which the relaxation time is comparable or much greater than the quench time scale so that the system evolves diabatically.

in the conduction bands and holes in the valence bands) in quantum Hall states are analogues to vortices and anti-vortices in the superfluid in this mapping, which are the topological defects of the ordered phase. In retrospect this is rather natural as the topological characterization is specific to the ground state; any excitation on top of the ground state causes deviation from, say the perfectly quantized Hall conductance of the ground state, and is clearly a topological defect. Thus, the excitations induced by the quenches through topological phase transitions are analogues to the those in ordered phases. This allows us to use the results of KZ theory (Eq. 3) on Haldane and checkerboard models as we are turning to now.

Due to linear quench, the gap has a linear dependence on the quench parameter in both Haldane and checkerboard models giving $z\nu = 1$ (according to $\Delta \sim |\mu - \mu_c|^{z\nu}$ where Δ is the gap and μ is the quench parameter.) For Haldane model which has $d = 2$ and $z = 1$ (linear dispersion) and $\nu = 1$, the predicted power α is 1 from KZ theory ($n_{topo} \sim \tau^{-\alpha}$); for checkerboard model whose $d = 2$, $z = 2$ (quadratic dispersion) and $\nu = \frac{1}{2}$, it gives $\alpha = 0.5$.

B. Landau-Zener (LZ) theory

LZ theory describes the dynamics of a two-level system with a time-dependent Hamiltonian in which the energy gap of the two states varies linearly with time. Note that LZ theory can be applied to such a two-level system regardless of the topology (trivial or non-trivial) of the states. Suppose that the Hamiltonian evolves with time t, from $t = -\infty$ to $t = +\infty$ in which the gap of the two states has a minimum at $t = 0$ (one can always shift the time such that the gap minimum occurs at $t = 0$) and that initially (at $t = -\infty$) one of the states is occupied and the other is empty. The Hamiltonian with the basis (ψ_+, ψ_-) can be written as

$$H = \begin{pmatrix} \epsilon_1 & \epsilon_{12} \\ \epsilon_{21} & \epsilon_2 \end{pmatrix} \tag{7}$$

where ψ_+ and ψ_- represent the two states with $\psi_+ = \begin{pmatrix} 1 \\ 0 \end{pmatrix}$ which is occupied and $\psi_- = \begin{pmatrix} 0 \\ 1 \end{pmatrix}$ which is empty at $t = -\infty$; ϵ_1 and ϵ_2 are the energies of the two states, and ϵ_{12} and ϵ_{21} correspond to the interaction between the two states. According to the Ref[7], the transition probability from ψ_+ to ψ_- will be

$$\Gamma\left(\vec{k}\right) \sim e^{\frac{-\pi}{2\hbar\Delta_{\vec{k}}}} \tag{8}$$

with $\Delta_{\vec{k}}^{-1} = \frac{4\epsilon_{12}^2}{|\frac{d}{dt}(\epsilon_1 - \epsilon_2)|}$. With the transition rate, the excitation density can be estimated through the integral of the probability over the first brillouin zone, namely, $n_{topo} \sim \int_{1BZ} d^d \vec{k} \, \Gamma\left(\vec{k}\right)$.

For Haldane and checkerboard models we consider here, two free fermion models, the many-body problems can be reduced to one-body problems since the eigenstates of the many-body Hamiltonian must be the Slater determinant of the single-particle states. Besides, with full translation symmetry, there are two good quantum numbers, namely the two components of the 2D momentum $\vec{k}$. Associated with two sublattices, Haldane model and checkerboard model, therefore, become collections of two-level systems (one for each $\vec{k}$) so the LZ theory, which considers a transition of two levels, can be applied. As we mentioned earlier, the particles in the conduction bands and holes in the valence bands generated by the quench process are the topological defects in our models thanks to the analogy between the quantum Hall effect and superfluidity. In the following, we will apply LZ theory on both Haldane and checkerboard models and compare with the results of KZ theory.

For Haldane model near K (or K') point where the gap closes at critical time, the low-energy Hamiltonian reduces to

$$H_K\left(\vec{k}\right) = \begin{pmatrix} m(t) + \bar{\eta} & v_f \, k \, e^{-i\phi} \\ v_f \, k \, e^{i\phi} & -m(t) - \bar{\eta} \end{pmatrix} \tag{9}$$

where $m(t) = \frac{t}{\tau}$ with $\frac{1}{\tau}$ the quench rate, $\bar{\eta}$ is a constant, v_f is the velocity of particles near K (or K') point and $\vec{k} = ke^{-i\phi}$ is the 2D momentum. Note that the linear dependence of $|\vec{k}|$ in the off-diagonal matrix elements captures the property of the linear dispersion near K (or K') point. As a result, the transition rate of the two energy levels $\Gamma\left(\vec{k}\right) \sim e^{\frac{-\pi v_f^2 |\vec{k}|^2 \tau}{\hbar}}$ gives the topological defect density $n_{topo} \sim \int d\vec{k} \, \Gamma\left(\vec{k}\right) \sim \frac{\hbar}{v_f^2 \tau} \propto \tau^{-1}$, a power-law relation with the same power as KZ theory predicts.

For checkerboard model, setting $\xi' = -\xi'' = 0.5$ to simplify the calculation without loss of generality, the Hamiltonian near the gap-closing point $\bar{K} = (k_x, k_y) = (\pi, \pi)$, after a unitary transformation such that it satisfies the initial condition LZ theory requires, that one band is fully occupied and the other is empty, can be expressed as

$$H_{\bar{K}}\left(\vec{k}\right) = \begin{pmatrix} -V & \frac{-i}{4} k^2 e^{2i\theta} \\ \frac{i}{4} k^2 e^{-2i\theta} & V \end{pmatrix} \quad (10)$$

where $\vec{k} = k e^{i\theta}$ and $V = \frac{t}{\tau}$. In this model, the off-diagonal matrix elements have quadratic dependence of $|\vec{k}|$ due to the quadratic band structure near the band touching point. Thus, the transition rate $\Gamma\left(\vec{k}\right) \sim e^{\frac{-\pi \tau k^4}{16\hbar}}$ and $n_{topo} \sim \tau^{-0.5}$, which also agrees with the prediction of KZ theory.

IV.   QUENCH DYNAMICS WITH EDGES

The presence of edges breaks translation symmetry at least in one direction, and we can no longer reduce the problem to a collection of two-level systems anymore. Instead we numerically study the slow quench process in the two models by considering strips infinitely long in the y direction having finite width in the x direction with open boundary conditions (OBCs), keeping k_y as a good quantum number.

Initially, we prepare the system in the ground state of the initial Hamiltonian H_0 and consider the half-filling case in which the lower bands are filled. During the slow quench process, we divide the whole process into many time periods such that the Hamiltonian $H(t)$ barely changes during each period Δt. From t to $t + \Delta t$, the eigenstate of $H(t)$ evolve approximately with a phase $e^{-i \frac{E_\alpha(t)}{\hbar} \Delta t}$ where E_α is the corresponding eigenenergy. Taking advantage of the simple evolution of the instantaneous eigenstates, we expand the wave function by the set of the instantaneous eigenstates of $H(t)$ so that the evolution of the wave function from t to $t + \Delta t$ could be expressed as $\psi_\beta(t + \Delta t) = \sum_\alpha e^{-i E_\alpha(t) \Delta t / \hbar} |\phi_\alpha(t)\rangle \langle \phi_\alpha(t) | \psi_\beta(t)\rangle$ where β labels the β-th eigenstate of H_0 and $|\phi_\alpha(t)\rangle$ and $E_\alpha(t)$ represent the α-th eigenstate of $H(t)$ and the corresponding eigenenergy. At the end of the quench process, we count the contribution of the initial states to each eigenstate of the final Hamiltonian H_f.

V.   NUMERICAL RESULTS

A.   Bulk excitation

In order to test the numerical accuracy, we first follow the quench evolution with periodic boundary conditions
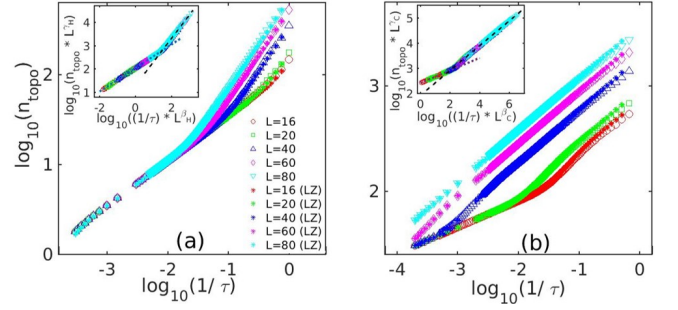

FIG. 4. (Color online) Topological excitation density versus quench rate in log-log plot in (a) Haldane model and (b) checkerboard model. Considering strips infinitely long in the y direction having L sites in the x direction with PBC (no edge), our data and the results from Landau-Zener (LZ) theory are shown for comparison. We perform finite-size scaling on our data such that $n'_{topo}\left(\tau^{-1} \cdot L^{\beta_a}\right) = L^{\gamma_a} n_{topo}\left(\tau^{-1}\right)$ is size independent in the insets with β_a and γ_a the scaling parameters and a the model label (H for Haldane model and C for checkerboard model.) According to LZ theory, $\tau_a^{-1} \sim k^{\beta_a} \sim L^{-\beta_a}$ with $\beta_H = 2$ and $\beta_C = 4$. Besides, $n_{topo} \sim L^{-1}$, meaning $\gamma_H = \gamma_C = 1$. Our fitting scaling parameters are $\beta_H = 1.9332$, $\gamma_H = 0.9701$, $\beta_C = 4.2266$ and $\gamma_C = 1.063$ consistent with the scaling analysis. The black lines are the fitting lines for the powers α. (a) In Haldane model, $\alpha = 1.0000$ in the (relatively) fast quench regime (slope of the dashed line) and $\alpha = 0.5008$ in the slow quench regime (slope of the dotted line); (b) In checkerboard model, $\alpha = 0.4925$ in the fast quench regime and $\alpha = 0.2502$ in the other regime. In each model, five systems with L = 16, 20, 40, 60, and 80 are considered.

(PBCs) applied in the x direction, instead of OBCs. In this case there is actually no edge and we can reduce the problem to two-level systems as discussed earlier. This allows us to compare our numerical results with those of the LZ theory (taking discrete k_x values for finite strips). In Fig. 4(a) and Fig. 4(b), our data in both models agree with LZ theory very well. Besides, we find that the excitation density n_{topo} and the quench rate $\frac{1}{\tau}$ have power-law relations with different powers αs in the (relatively) fast quench and slow quench regimes; α in the fast quench regime agrees with the theoretical value KZ and LZ theories predict, but it becomes half of the expected value in the slow quench regime. In the inset of Fig. 4(a) for Haldane model, α (slope) at fast quenches is 1.0000 and becomes 0.5008 at slow quenches; in the inset of Fig. 4(b) for checkerboard model, α is 0.4925 and 0.2502 in the fast and slow quench regimes, respectively. The halved powers in the slow quench regime are due to finite-size effect. For systems with finite width in the x direction, the k_x takes discrete values so that the transition occurs dominantly at $k_x = 0$ if we shift the critical point to the origin; at other k_x values far from the origin, the dynamics is adiabatic. Therefore, the diabatic dynamics becomes 1D (along k_y at $k_x = 0$) leading to an exponent halved from that of the 2D system.
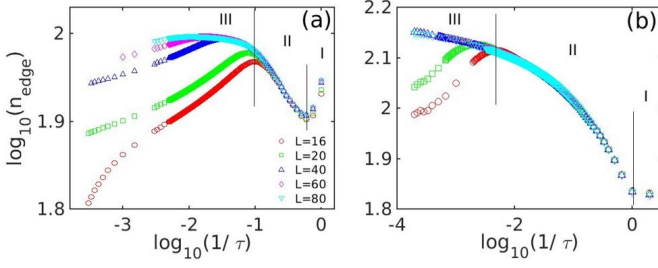
FIG. 5. (Color online) Edge excitation vs quench rate in log-log plot for (a) Haldane model with zigzag edges. (b) Checkerboard model. System sizes: L = 16, 20, 40, 60 and 80 are considered.
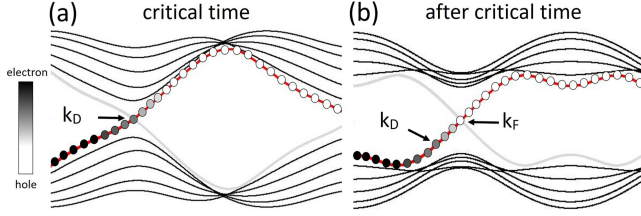

FIG. 6. (Color online) Schematic diagrams for electron occupation of one branch of edge states (a) at the critical time and (b) after the critical time. The light gray curve is the other edge state which could be ignored in the quasi-adiabatic regime due to the lack of edge state mixing. k_D and k_F denote the Fermi energy locations at the critical time and at some moment after the critical time, respectively.
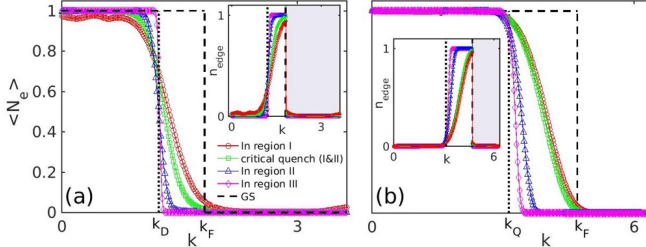

FIG. 7. (Color online) Electron occupation along k with different quench rates for (a) Haldane model (b) checkerboard model. The dotted lines mark k_D or k_Q (the Fermi level location at the critical time for Haldane and checkerboard models respectively) and the dashed curves represent the electron occupation of the edge state in the ground state. The insets show the edge excitation n_{edge} corresponding to each quench rate. The edge excitations in the shaded area are particle excitations and are hole excitations otherwise.

B. Edge excitation and excitation generation mechanism

Now turning to the cases with edges, we consider strips with OBCs and zigzag edges for Haldane model. Since now k_y is the only good quantum number, we will simplify the notation by using k for k_y in the following. In the presence of edges, a system will have edge states in a topologically non-trivial phase. If the system were in

the ground state for half-filling case, the bands below the fermi energy E_F would be all occupied and the others would be all empty. Since edge states cross the bulk gap, the electron occupations on edge states in the ground state take the form of a step function $\Theta(E_F - E)$, where $\Theta(x) = 1$ for $x > 0$ and $\Theta(x) = 0$ otherwise. Under a quench process, however, the system can not evolve adiabatically near the critical time and hence can not stay in the ground state. Instead, excitations will be generated both in the bulk and on the edge states. We can expand the eigenstates of the final Hamiltonian H_f through those of the initial Hamiltonian H_0 (half-filling) at each k as $|\psi(k)\rangle_\alpha^{(f)} = \sum_{\beta=1}^L \omega_{\alpha\beta}(k)|\psi(k)\rangle_\beta^{(0)}$ where $|\psi(k)\rangle_\alpha^{(f)}$ and $|\psi(k)\rangle_\beta^{(0)}$ denote the αth and βth eigenstates of H_f and H_0, respectively, with $\omega_{\alpha\beta}(k) = {}_\beta^{(0)}\langle\psi(k)|\psi(k)\rangle_\alpha^{(f)}$; L is the width in the x direction (so there are L states.) Assume the states have energies in ascendant order, namely, $E_1^{(i)} < E_2^{(i)} < \cdots < E_L^{(i)}$ with $i = f$ and 0. The edge states of H_f are $|\psi(k)\rangle_{L/2}^{(f)}$ and $|\psi(k)\rangle_{L/2+1}^{(f)}$, and the (total) edge excitations n_{edge} can be defined as

$$n_{edge} = \sum_{\alpha=L/2}^{L/2+1} \int dk \, [\, \sum_{\beta=1}^{L/2} |\omega_{\alpha\beta}(k)|^2 \Theta(\, E_\alpha^{(f)}(k) - E_F^{(f)}\,)$$
$$+ \sum_{\beta=L/2+1}^{L} |\omega_{\alpha\beta}(k)|^2 \Theta(\, E_F^{(f)} - E_\alpha^{(f)}(k)\,)\,],$$
(11)

the deviation of the electron occupations on edge states from their ground state occupations at the end of the quench. In Fig. 5(a) and Fig. 5(b), we investigate n_{edge} with various quench rates and find distinct behaviors in three regimes of the quench rate. In regime I, n_{edge} decays with quench rate decreasing, consistent with the physical intuition. In regime II, unexpectedly n_{edge} increases as quench rate decreases, displaying an anti-KZ behavior. In regime III, it seems to obey KZ mechanism again.

To understand the behaviors of n_{edge} especially the anti-KZ behavior, we examine the formation and evolution of the edge states, starting with the moment when the band gap closes and edge states just begin to form in Haldane model. At the critical time, conduction and valence bands strongly mix near the band gap closing point (k_D) and form edge states. Except for the slowest quench rate that we will comment on later, we can ignore the coupling between states on opposite edges and focus on one branch of the edge states, pretending the other edge does not exist. We can schematically express the branch of edge states of interest as $\psi_{edge}(k) = a(k)\psi_c(k) + b(k)\psi_v(k)$ where ψ_c and ψ_v denote the contributions from conduction and valence bands before the gap closing, respectively, and $a(k)$ and $b(k)$ represent the corresponding weights, depending on k but not the quench rate, with $a^2(k) + b^2(k) = 1$. As illustrated in Fig. 6(a), edge states with $k < k_D$ are predominantly from valence bands, while

those with $k > k_D$ are predominantly from conduction bands. This feature is expected to persist as the gap opens up, as illustrated in Fig. 6(b). We now introduce a regime of "quasi-adiabatic" time-evolution after the gap opens, namely the quench rate is small enough such that there is no transition between edge states and bulk states, but fast enough so that edge states remain at the *same* edge, namely an edge state at one edge does not evolve into the other at the opposite edge with the same k when their energies cross. For sufficiently wide strips such a regime is guaranteed to exist as the coupling between the edges is exponentially suppressed. In this regime the occupation number of an edge state is well-approximated by $b^2(k)$ at the point of gap closing, which is close to one for $k < k_D$ and close to zero otherwise. With the gap opening up, however, the Fermi wave vector k_F increases (see Fig. 6(b)), resulting in significant numbers of hole-like edge excitations for $k_D < k < k_F$. On the opposite edge we expect equal numbers of particle-like excitations. Increasing the quench rate induces relaxations of the edge excitations into the bulk, giving rise to the anti-KZ behavior. Further increasing the quench rate, on the other hand, induces additional edge excitations, especially outside the range $k_D < k < k_F$. This brings us back to the usual KZ behavior. Fig. 7(a) and Fig. 7(b) show the electron occupation distribution of one edge state along k in different quench regimes and the insets show the dominance of hole excitations on this edge state, supporting our argument.

Finally, the KZ behavior in regime III is due to essentially true adiabatic evolution in which edge states on opposite edges are mixed. This is a finite-size effect due to the exponentially small coupling between the edges. Consistent with this understanding, we find it is more prominent in small systems as shown in Figs. 5. In the thermodynamic limit, without the particle leaking from edges, the edge excitation numbers will eventually saturate in the slow quench, instead of going to zero as we observed at finite strip width.

VI. CONCLUSION

We numerically study the dynamics of Haldane model and checkerboard model in slow quench processes through topological quantum phase transitions with $\Delta C = 1$ and 2, respectively. We show the agreement of the power-law relations of the bulk excitation and the quench rate with the predictions of KZ and LZ theories. Besides, an anti-KZ behavior of the edge excitation is found in both models. We provide a physical picture for this counter-intuitive feature which originates from the unrelaxable nature of excitations on edge states since the edge states form.

[1] T. W. B. Kibble, J. Phys. **A 9**, 1387 (1976).

[2] T. Kibble, Phys. Rep. **67**, 183 (1980).

[3] W. H. Zurek, Nature (London) **317**, 505 (1980).

[4] W. H. Zurek, Phys. Rep. **276**, 177 (1996).

[5] A. Chandran, A. Erez, S. S. Gubser, and S. L. Sondhi, Phys. Rev. B **86**, 064304 (2012).

[6] W. H. Zurek, U. Dorner, and P. Zoller, Phys. Rev. Lett. **95**, 105701 (2005).

[7] C. Zener, Proc. R. Soc. London, Ser A **137**, 696 (1932).

[8] B. Damski, Phys. Rev. Lett. **95**, 035701 (2005).

[9] J. Dziarmaga, Phys. Rev. Lett. **95**, 245701 (2005).

[10] J. Dziarmaga and M. M. Rams, New Journal of Physics **12**, 055007 (2010).

[11] D. Sen, K. Sengupta, and S. Mondal, Phys. Rev. Lett. **101**, 016806 (2008).

[12] R. Barankov and A. Polkovnikov, Phys. Rev. Lett. **101**, 076801 (2008).

[13] F. D. M. Haldane, Rev. Mod. Phys. **89**, 040502 (2017).

[14] C.-X. Liu, X.-L. Qi, X. Dai, Z. Fang, and S.-C. Zhang, Phys. Rev. Lett. **101**, 146802 (2008).

[15] C.-Z. Chang, W. Zhao, D. Y. Kim, P. Wei, J. K. Jain, C. Liu, M. H. W. Chan, and J. S. Moodera, Phys. Rev. Lett. **115**, 057206 (2015).

[16] A. Bermudez, D. Patanè, L. Amico, and M. A. Martin-Delgado, Phys. Rev. Lett. **102**, 135702 (2009).

[17] A. Bermudez, D. Patanè, L. Amico, and M. A. Martin-Delgado, New J. Phys. **12**, 055014 (2010).

[18] M. Lee, S. Han, and M.-S. Choi, Phys. Rev. B **92**, 035117 (2015).

[19] A. A. Patel, S. Sharma, and A. Dutta, Eur. Phys. J. B **86**, 367 (2013).

[20] M. D. Caio, N. R. Cooper, and M. J. Bhaseen, Phys. Rev. Lett. **115**, 236403 (2015).

[21] M. D. Caio, N. R. Cooper, and M. J. Bhaseen, Phys. Rev. B **94**, 155104 (2016).

[22] C. Wang, P. Zhang, X. Chen, J. Yu, and H. Zhai, Phys. Rev. Lett. **118**, 185701 (2017).

[23] M. Tarnowski, F. N. Unal, N. Flaschner, B. S. Rem, A. Eckardt, K. Sengstock, and C. Weitenberg, arXiv:1709.01046 (2017).

[24] M. S. Foster, M. Dzero, V. Gurarie, and E. A. Yuzbashyan, Phys. Rev. B **88**, 104511 (2013).

[25] M. S. Foster, V. Gurarie, M. Dzero, and E. A. Yuzbashyan, Phys. Rev. Lett. **113**, 076403 (2014).

[26] Y. Liao and M. S. Foster, Phys. Rev. A **92**, 053620 (2015).

[27] A. Chandran, F. J. Burnell, V. Khemani, and S. L. Sondhi, Journal of Physics: Condensed Matter **25**, 404214 (2013).

[28] P. D. Sacramento, Phys. Rev. E **90**, 032138 (2014).

[29] G. Jotzu, M. Messer, R. Desbuquois, M. Lebrat, T. Uehlinger, D. Greif, and T. Esslinger, Nature **515**,

237 (2014).

[30] F. D. M. Haldane, Phys. Rev. Lett. **61**, 2015 (1988).

[31] K. Sun, H. Yao, E. Fradkin, and S. A. Kivelson, Phys. Rev. Lett. **103**, 046811 (2009).

[32] K. Sun, Z. Gu, H. Katsura, and S. Das Sarma, Phys. Rev. Lett. **106**, 236803 (2011).

[33] S. C. Zhang, Int. J. Mod. Phys. **B 6**, 25 (1992).